Light and Electron Microscopic Studies of the Rat Kidney After Administration of Inhibitors of the Citric Acid Cycle In Vivo

I. Effects of Sodium Fluoroacetate on the Proximal Convoluted Tubule

Elizabeth M. McDowell, PhD

Light and electron microscopic studies of morphologic changes in the rat proximal convoluted tubule after intraperitoneal injection of sodium fluoroacetate (FAc), 60, 20 and 3.5 mg/kg body weight, have been made. Particular attention was directed toward appreciating different changes in the first (S_1) and second (S_2) segments of the proximal tubule. The earliest change was loss of mitochondrial granules and pallor of the mitochondrial matrix, not necessarily associated with matrix swelling. Matrix swelling was greatest at 3 hours after 3.5 mg/kg and was reversible. However, the mitochondria retained their elongate shape and cristae persisted. At 48 hours, some mitochondria appeared normal; in others, abnormal matrix densities of unknown nature were present. Mitochondrial changes were similar in S_1 and S_2 at all times. Enlarged apical vacuoles, most pronounced in S_1, occurred in all rats after 20 mg/kg. The change was uncommon after 3.5 mg/kg. The hypothesis proposed is that vacuoles arise during an FAc-induced hyperglycemic phase, when pinocytotic activity is maintained but the normal pathway of glucose catabolism is inhibited. Moderate dilatation of the rough-surfaced endoplasmic reticulum occurred during the first 2-hour period in S_1 and S_2 tubules after high and low doses, but between 6 and 24 hours, dilatation was extensive in S_1 tubules after 3.5 mg/kg. This change was reversible. Two types of abnormal vacuolar bodies, large and small, have been described, and were unique to S_1 tubules. Acid phosphatase activity was demonstrated in a proportion of the small ones, indiciating that they were a type of lysosome. The larger ones shared features in common with cytosomes of control cells, but acid phosphatase activity was not demonstrated in them and their origins and functions remain obscure. The biochemical lesions induced by fluoroacetate have been discussed and a tentative interpretation of some of the morphologic changes has ben made (Am J Pathol 66:513–542, 1972).

A COMPARATIVE MORPHOLOGIC STUDY has been made of the sequence of changes that occur in the kidneys of rats poisoned by single doses of three agents that block the citric acid cycle *in vivo*.[1] The present paper describes morphologic changes that occurred in the proximal

From the Department of Pathology, University of Cambridge, Cambridge, England.
Supported by a food safety training scholarship from the Nuffield Foundation.
Accepted for publication September 7, 1971.
Present address of Dr. McDowell is the Department of Pathology, University of Maryland School of Medicine, Baltimore, Md 21201.

convoluted tubule during poisoning with sodium fluoroacetate ($FCH_2.COONa$).

Chenoweth [2] summarized the toxic effects of monofluoroacetates in many species; respiratory depression and tonic convulsive periods were characteristic symptoms in rats. After dosing with fluoroacetate (FAc), the citrate concentration rose in many tissues and was particularly high in the kidneys, up to 70 times normal values; [3,4] accumulation of citrate preceded toxic symptoms.[5] A fluorotricarboxylic acid was isolated from particle preparations of kidneys treated with FAc [6] and this was inhibitory to aconitase.[7] The inhibitory substance for citrate metabolism formed biosynthetically from FAc was considered to be fluorocitric acid; it inhibited the disappearance of approximately 300 times its weight of citric acid.[8]

Because the biochemistry of FAc poisoning has been studied extensively, it was of interest to study the morphologic effects of this mitochondrial poison in the proximal convoluted tubule, a tissue known to be highly dependent on oxidative respiration.

Materials and Methods

The kidneys of 50 young Hooded Lister rats of both sexes, weighing between 120 and 300 g were examined; of these, 10 served as controls (Table 1). The rats received a standard cube diet and water *ad libitum* up to the start of the experiments. Sodium fluoroacetate (fluoride-free) was given intraperitoneally, either

Table 1—Fixation Schedule

Total No.	Sex	Control	FAc (mg/kg)	No. of rats at each time interval (hours after dosing)									
				½	1	1½	2	3	6	12	24	48	72
Test													
9	M			1	1		1	1	1	1	1	1	1
			3.5										
10	F			1	1		2	1	1	1	1	1	1
11	M			2	3	3	3						
			20										
7	F			3	2	2	(3)*						
1	M				1								
			60										
2	F				2								
Control													
5	M			1	1		1		1			1	
		Saline											
5†	F			1	1		1				1		

* Rats died before 2 hours.

† One control rat received no treatment.

as an isotonic aqueous solution (0.15 M) or in 0.5 or 1.0 ml of sterile physiologic saline at 3.5, 20 and 60 mg/kg body weight. These doses were chosen because they are similar to doses used previously by others in biochemical studies. Control rats received saline; 1 rat received no treatment (Table 1).

After light ether anesthesia, the test or control solution was injected. Additional anesthesia, pentobarbital sodium, was given intraperitoneally.

When sufficient volume was present, urine was withdrawn from the bladder just before perfusion fixation. Urine pH and the presence of blood, glucose and protein was tested with Hema-combistix reagent strips (Ames Co, United Kingdom). The test for glucose is specific but is only semiquantitative. A "light" positive indicates 0.25% glucose or less and "dark" indicates 0.5% or more. Ketonuria was tested with Acetest reagent tablets (Ames Co).

All kidneys were fixed by intravascular perfusion of 2.5% glutaraldehyde in Veronal acetate buffer, pH 7.2 [9] at near-physiologic blood pressure, according to the method described by Griffith *et al.*[10]

Light Microscopy

Portions of both kidneys were postfixed in formol saline, dehydrated in alcohols and embedded in paraffin; 5.0-μ thick sections were stained with hematoxylin and eosin (H&E) and by the periodic acid–Schiff method (PAS). Glutaraldehyde provides free aldehyde groups which react with Schiff's reagent.[11] To overcome this, sections were brought to water and soaked in saturated aqueous Dimedone (British Drug Houses, Ltd, United Kingdom) for 24 hours before staining. The chloranilic acid method for calcium [12] was employed on sections of kidneys after 3.5 mg/kg FAc and on appropriate control sections.

Fat was demonstrated in 10-μ-thick, fixed frozen sections of selected control and test tissue by the Sudan III and IV method.

Electron Microscopy

After perfusion fixation, 1-mm cubes of cortex were postfixed in 2.5% glutaraldehyde for 2–48 hours at 4 C, followed by 2 hours in 2% OsO_4 in Veronal acetate buffer. Contrast was enhanced in thin sections by soaking the blocks in 0.5% uranyl acetate in Veronal acetate buffer before dehydration; [13] tissue cubes were soaked for 16 hours to ensure complete penetration before dehydration in alcohol, starting at 70%. Tissue was embedded in Araldite. Thick (0.5–1.0-μ thick) and thin sections were cut with glass knives on a Huxley ultramicrotome (Cambridge Instrument Co, Ltd, United Kingdom). Thick sections were stained with alkaline toluidine blue solution for light microscopy.[14] Thin sections were mounted on uncoated copper grids and stained with lead citrate [15] before examination in a Siemens Elmiskop Ib electron microscope.

Acid phosphatase activity (APase) was demonstrated at light and electron microscopic levels in kidneys of 2 rats at each time interval after receiving FAc, 20 mg/kg, and in those of 4 control rats. For electron microscopy, 1-mm cubes were postfixed in 3% Veronal acetate–buffered glutaraldehyde, with 5% sucrose, for 2–3 hours at 4 C. After an overnight wash in sucrose buffer at 4 C, 50-μ thick sections were cut on a freezing microtome. Sections were incubated for 12–15 minutes at 37 C in the incubation medium,[16] which was prepared 2 hours before use. Control sections were incubated in complete medium to which 10^{-2} M sodium fluoride had been added. Preparation for electron microscopy was as described above. For light microscopy, 10-μ-thick frozen sections were incubated in the medium [16] for 1 hour at 37 C and treated with dilute ammonium sulfide.

Results

Control

Urine Tests

Blood, glucose and ketone bodies were absent. The urine of some male rats had a moderate proteinuria, 30 mg/100 ml.

Light Microscopy

Abnormalities were not seen in control sections. Morphologic differences between the first and second segments of the proximal convoluted tubules, S_1 and S_2,[17] were obvious in toluidine blue-stained Araldite sections (Fig 1). Neck segments, those parts of S_1 in continuity with the glomerular capsule, and S_1 tubules had wide brush borders and elongate mitochondria arranged perpendicular to the basement membrane. The number and size of apical vacuoles were comparable in S_1 and S_2 tubules, but S_2 was clearly recognizable by more numerous densely stained cytoplasmic bodies, which were especially large in male rats.

Electron Microscopy

Detailed descriptions of the fine structure of cells of the proximal convoluted tubule of the rat,[18–20] and of the localization of APase,[21–26] have been made, and the appearance of control cells in this study was comparable with that described previously. Apical tubular invaginations were present between bases of microvilli and numerous apical vesicles, and apical dense tubules were present in the aprical cytoplasm.[19,21] Larger apical vacuoles, up to 2.0 μ in diameter, were seen below the level of apical vesicles, and, not infrequently, dense floccular material was located towards the periphery of their translucent content (Fig 5).

Single-membrane-bound cytoplasmic bodies with APase have collectively been called "cytosomes"[24] and this terminology will be adopted in the absence of precise measurements of membranes required for the classification advocated by Maunsbach.[26] Cytosomal heterogeneity was observed, as described previously,[24,26] but cytosomes with pale matrices were not common in S_1 tubules, as described in Sprague-Dawley rats using a similar fixation procedure,[17,26] and many S_1 cytosomes appeared dense (Fig 5); varying amounts of layered material lay within them and small areas of increased density were often seen in the matrix (Fig 6). APase was demonstrated in cytosomes, but reaction product was not associated with all of them and in some, it was sparse.

The mitochondrial matrix had considerable electron density when

stained with uranyl acetate and lead citrate; dense matrix granules were present in control mitochondria (Fig 6). Ribosomes in polysome groups were dispersed throughout the cytoplasm and small chains of rough-surfaced endoplasmic reticulum (RER) lay scattered in the cytoplasm; the cisternae were not dilated (Figs 5 and 6).

The nuclei tended to be elliptic and the perinuclear cisterna was not dilated (Fig 5). Aggregation and margination of chromatin, a feature of primary aldehyde fixation [27] was seen in the nuclear sap and at the periphery, except at the nuclear pores (Fig 5).

Fluoroacetate Poisoning

General Condition of Poisoned Rats

Hooded Lister rats were relatively tolerant of FAc and although very toxic, none of the rats died before the scheduled time of killing after receiving 3.5 mg/kg. The LD_{50} for FAc in Holzman rats was quoted as 1.0–2.0 mg/kg over 24 hours.[28] Strain variations have been reported.[2] After 3.5 mg/kg, the rats huddled in cage corners, disinclined to move, their coats were staring and their extremities felt cold to the touch. Approximately one-half of the rats had convulsions between 1 and 4 hours after dosing. At 24 hours, the rats were brighter and by 36 hours, those that had been very ill were playing with their cage mates. Male rats appeared to be more resistant to 20 mg/kg than were female rats, as none of the latter survived after 90 minutes (Table 1); tonic convulsions occurred in 1 rat at 1 hour.

Urine Tests

Hematuria, proteinuria and ketonuria did not occur and pH values were comparable with control values. Medium-to-dark positive glycosuria was recorded in approximately 50% of the 1-hour samples and in all later samples after 20 mg/kg. Glycosuria did not occur after 3.5 mg/kg, with the exception of a light positive in one 12-hour sample.

Light Microscopy

The morphologic changes occurring in the kidneys after the high doses of the FAc are described before those occurring after the low dose because, during the early time intervals, many changes were comparable at all dose levels.

Paraffin and Frozen Sections. Apart from an increase in the number and size of apical vacuoles at 1 and 2 hours after 20 mg/kg, the tubules appeared normal. Changes in the distribution of APase were not observed.

The tubules appeared unchanged up to 6 hours after 3.5 mg/kg, but at 12 hours the cytoplasm of the neck segments was more eosinophilic than normal and foamy. Many tubules, presumably S_2, appeared unchanged. Fat droplets were seen at 12 and 24 hours. The tubules appeared normal at 48 and 72 hours; calcium deposition did not occur.

Araldite Sections Stained with Alkaline Toluidine Blue Solution. 20 MG/KG. Between 30 minutes and 1 hour, enlarged unstained apical vacuoles were seen in neck and S_1 tubules (Fig 2). At 90 minutes, many measured 6.0 μ in diameter and by 2 hours they lay two and three deep (Fig 3). Vacuolar bodies, 1.0–2.0 μ in diameter, distinct from the apical vacuoles and characterized by a pale blue-stained periphery and a central densely stained "nucleoid," were seen midcell in S_1 tubules from 1 hour onward (Fig 2). Normal dense cytoplasmic bodies persisted in the cells and enlarged pale-staining cytoplasmic bodies were not seen. The same changes were observed at 1 hour after 60 mg/kg.

Apical vacuoles increased in size in S_2, but to a lesser extent, their diameter not exceeding 3.0 μ. They remained in the apical regions even at 2 hours (Fig 3). Vacuolar bodies with "nucleoids" were not seen in S_2.

Cell volume, cytoplasmic density, nuclei and mitochondria appeared unchanged in both segments. Sex differences were not observed.

3.5 MG/KG. With the exception of 2 rats during the first 3 hours, a marked increase in the size of apical vacuoles did not occur, although a slight increase was seen in all rats during the first 24 hours. Some midcell vacuolar bodies with "nucleoids" were seen in S_1 tubules between 1 and 2 hours and at 12 hours, when they were numerous, the number of dense cytoplasmic bodies appeared to be reduced. Cytoplasmic pallor and moderate cell swelling occurred in 2 rats at 2 hours, but this change was atypical. At 3 and 6 hours, the cytoplasm of some tubules appeared white-flecked and at 12 hours, focal areas of marked vacuolation were confined to neck and S_1 tubules (Fig 4), corresponding to the foamy neck segments seen in H&E-stained sections. Vacuolation was also marked in distal tubules and the media of small arteries [1] but was absent from S_2 tubules. The extent of the vacuolation had decreased by 24 hours, nuclear changes were not seen and necrosis did not occur. Abnormalities were not seen at 48 and 72 hours.

Electron Microscopy

20 MG/KG. The changes are summarized in Table 2. At 30 minutes, mitochondrial matrix density was reduced in some cells and matrix granules were absent. At 1 and 2 hours, all mitochondria were affected;

Table 2—Changes in the First (S_1) and Second (S_2) Segments of the Proximal Convoluted Tubules During Fluoroacetate Poisoning (20 mg/kg)*

Time (hr)	Increase in size and No. of apical vacuoles		Mitochondria	ASMBV†	Dilatation of RER	Ring forms
	S_1	S_2	S_1 and S_2	S_1 S_2	S_1 and S_2	S_1 S_2
½	+	+	Matrix pallor,			
1	++	+	absence of	+	+	+
1½	+++	+		+	+	+
2	+++	+	matrix granules	+	+	+

* Blanks indicate no abnormality. Changes were not seen in cytosomes, microbodies, nuclei or cell volume.

† Abnormal single-membrane-bound vacuoles, small and large.

in some cells they were a little swollen but matrix pallor was not necessarily associated with swelling (Fig 7). Mitochondrial changes were similar in S_1 and S_2 at all times and abnormal matrix densities were not seen during the 2-hour period. Normal cristal architecture was largely retained but some cristae appeared angulated (Fig 7).

At 1 hour the number and size of apical vacuoles had markedly increased in S_1 cells (Fig 8); they enlarged by fusion (Fig 8, 10 and 17) and at 2 hours often lay three-deep (Fig 17). APase was not demonstrated within them (Figs 11 and 12). Single-membrane-bound bodies containing a few vesicles lay near to and possibly fusing with the vacuoles (Fig 8); APase was not demonstrated within these bodies (Fig 12). Normal cytosomes were retained in S_1 cells (Fig 8, 9, 11, 12 and 17) and conclusive evidence of fusion with apical vacuoles was lacking. An obvious reduction in the numbers of cytosomes was not apparent.

Abnormal single-membrane-bound vacuolar bodies were seen at mid-cell level in S_1 tubules from 1 hour onward; they were classified according to size. Those measuring 0.6–2.0 μ in diameter were called large (Fig 9, 10 and 13). They were characterized by a central dense area, the "nucleoid," which was surrounded by an outer zone of looser floccular material. A translucent peripheral zone separated the latter from the membrane. Focal areas of increased density within the nucleoid (Fig 9) and varying amounts of layered material (Fig 10) were features in common with normal cytosomes, but APase was not demonstrated within them (Fig 11). Close association between a large vacuolar body and enlarged apical vacuoles is shown in Figure 10, indicating that fusion was imminent. Abnormal vacuoles, measuring 100 to 600 mμ in diameter were called small; they appeared in groups near the Golgi apparatus. Their matrix had moderate electron density and was surrounded by a

translucent zone of varying width (Fig 13); APase was demonstrated in a proportion of them (Fig 14). Morphologically similar bodies were rarely seen near the Golgi apparatus of control S_1 cells. Small vacuolar bodies were also seen in the apical cytoplasm, close to the enlarged apical vacuoles (Fig 8).

Apical vacuoles were increased in size and number in S_2 tubules but they rarely exceeded 2.5 μ in diameter. Abnormal vacuolar bodies were not seen in S_2 cells.

Moderate dilatation of the RER occurred at 1 hour in S_1 and S_2 cells and the density of the cisternal content was reduced but ribosomes remained attached to the membrane (Fig 8 and 9). Polysome groups tended to disperse by 90 minutes (Fig 10). The Golgi cisternae appeared unaltered, but spatially associated with the Golgi area of S_1 cells were ring forms consisting of double membranes separated by a narrow cisternal space of moderate electron density (Fig 9). Cytoplasm containing ribosomes was enclosed within the rings but mitochondria were not. APase was demonstrated in their cisternae (Fig 15) and similar ring forms were also seen in the apical cytoplasm (Fig 16).

Abnormalities were not seen in microbodies or nuclei apart from dilatation of the perinuclear cisternae. Normal cytoplasmic volume was maintained throughout the 2-hour period.

3.5 MG/KG. The changes are summarized in Table 3. Mitochondrial changes during the first 2 hours were similar to those after 20 mg/kg but at 3 and 6 hours, mitochondrial width had increased up to threefold in some cells (Fig 18). Although grossly enlarged apical vacuoles occurred in S_1 tubules of only 2 rats during the initial 3 hours, the distribution of abnormal midcell vacuolar bodies, large and small, was similar to the 20 mg/kg dose (Fig 18), and both types were seen to varying degrees in S_1 cells during the first 24 hours.

Between 1 and 6 hours, dilatation of the ER had occurred and was most marked in S_1 cells. The ribosomes had dislocated from the membranes and polysome groups had dispersed (Fig 18). The dilatation was extensive in S_1 cells at 12 and 24 hours (Fig 19 and inset), corresponding to the vacuolation seen in toluidine blue–stained sections (Fig 4). The mitochondria were not swollen and cytoplasmic volume was maintained. Fat droplets were seen at the bases of many cells (Fig 19). Dilatation of the ER was reversible, necrosis did not occur and at 24 hours many S_1 cells appeared normal, except for the absence of mitochondrial granules (Fig 20). In some cells, matrix granules had returned at 48 and 72 hours; in others, the matrix had low density, and irregular dense bodies were seen within it, displacing the cristae (Fig 21). Abnormalities in other organelles did not accompany this mitochondrial alteration.

Table 3—Changes in the First (S_1) and Second (S_2) Segments of the Proximal Convoluted Tubules During Fluoroacetate Poisoning (3.5 mg/kg)*

Time (hr)	Increase in size and No. of apical vacuoles		Mitochondria	ASMBV†		Dilatation of RER		Lipid droplets
	S_1	S_2	S_1 and S_2	S_1	S_2	S_1	S_2	S_1 and S_2
½	+	+	Matrix pallor,					
1	+‡	+	absence of	+		+	+	
2	+	+	matrix granules	+		+	+	
3	+‡	+	Matrix pallor and	+		++	+	
6	+	+	swelling, absence of matrix granules	+		+++	+	
12	+	+	Matrix density	+		++++	+	++
24	+	+	retained, not swollen, absence of matrix ganules	+		+++		++
48			Normal in some					
72			cells, abnormal matrix densities present in others					

* Blanks indicate no abnormality, changes were not seen in microbodies, nuclei or cell volume.

† Abnormal single-membrane-bound vacuoles, small and large.

‡ Apical vacuoles markedly increased in 1 rat (see text).

Discussion

Control

Segmental variations between S_1 and S_2 deviated slightly from those described by Maunsbach,[17] in that there was no appreciable difference between the size and number of apical vacuoles in S_1 and S_2 tubules and the cytoplasmic bodies of S_1 tubules were not predominately of the pale matrix type. This may represent a strain difference.

The Biochemical Lesion

The biochemical studies of previous investigators will be discussed and, where relevant, a tentative interpretation of morphologic changes will be made.

Accumulation of citrate in the kidneys is well established during FAc poisoning *in vivo*,[3,4,28–36] resulting from an inhibition of aconitase,[7] due to the biosynthetic formation of fluorocitrate (FC).[6,8] The inhibition of aconitase by biosynthetic FC was found to be competitive with citrate.[37] The fluoroacetates themselves have virtually no effect upon enzymes.[38] During FAc poisoning, citrate accumulates within the mitochondrial fraction,[39] citrate may leak into the cytoplasm to some extent but FC, formed by enzymic synthesis, is thought to remain bound within mitochondria.[40]

Potter *et al* [28] found that citrate concentrations in rat kidney rose with increasing dose and reached maximum levels between 3 and 6 hours after 3.5 mg/kg. Citrate levels were raised for up to 40 hours after a single low dose.[30]

Competitive inhibition of aconitase by FC is well established, but this probably represents only one factor responsible for the toxic effects. Seven labeled components were described in rat urine after a single dose of ^{14}C FAc.[32] High concentrations of the label were found in kidney mitochondria. The activity recovered as FC was similar after high and low doses of FAc, indicating that there is a limit to the amount of FC that can be produced. Only 32% of the label was excreted over 2–4 days, and radioactivity remained high in the kidneys. Label was incorporated into lower and higher fatty acids and indications were that fluorine was present.[32] Corsi and Granata [41] found that kidney mitochondrial oxygen consumption was lowered with citrate, pyruvate, β-oxobutyrate and L-glutamate as substrates, at 1 hour after 20 mg/kg FAc; succinate oxidation was reduced only at low substrate levels. Phosphorylation was not appreciably uncoupled, in agreement with studies made on liver and muscle,[42,43] but the respiratory control index was lowered.

It is clear that secondary changes in metabolism occur in the wake of the initial lesion. Hyperglycemia [44] together with ketonemia,[45] have been described. Phosphofructokinase (PFK) was inhibited in FAc-poisoned heart preparations,[46] simultaneous with an increased citrate concentration. Glucose uptake was decreased and the intracellular concentration of free glucose rose. Similar observations were made on heart poisoned *in vivo*.[47,48] The important regulatory role of citrate in cell metabolism is now well recognized.[49]

Mitochondrial Changes

Mitochondrial changes were similar after high and low doses. This is not surprising if mitochondrial conversion of FAc to FC is limited.[32] Loss of matrix granules, simultaneous with pallor of the matrix was the earliest change seen, followed by varying degrees of matrix swelling. It is generally accepted that the citric acid cycle enzymes are located in the matrix while succinic dehydrogenase is an integral part of the inner mitochondrial membrane.[50] When the cycle is inhibited by FC, citrate will accumulate, presumably within the matrix. Expansion of the matrix is associated with water uptake,[51] and water influx would be expected through the inner membrane to equilibrate osmotic pressures of the matrix and cytoplasmic compartments.[52]

Mitochondrial matrix granules may represent binding sites for cations,[53] Mg^{++} being the major cation.[54] Early loss of granules may be associated with solubilization of the cations, forming undissociable complexes with citrate. The significance of the change is not understood.[55]

Loss of respiratory control and loose coupling in FAc-poisoned kidney mitochondria has been discussed.[41] Angulated cristae, similar to those seen in some FAc-poisoned mitochondria, were described in heart mitochondria from a patient with hypermetabolism of nonthyroid origin.[56] These mitochondria had partial loss of respiratory control, matrix granules were absent and the matrix had low electron density.

The greatest degree of mitochondrial swelling occurred at 3 hours after 3.5 mg/kg, corresponding in time with the maximum citrate concentration reported by others.[28] The change was reversible. Abnormal matrix inclusions were not seen before 48 hours, were not associated with cristae and their significance and nature are unknown. It is possible that the inclusions represented FC, or a product thereof, perhaps in organic complex, as a high percentage of FC was retained in FAc-poisoned kidneys.[32]

Comments on Other Cell Components

Cell Sap

Swelling of the cytoplasm did not occur, with two exceptions, when swelling was moderate, indicating that energy levels were sufficient to maintain active transport essential for maintenance of normal cell volume.[57] In this regard, it is interesting to note that normal electrolyte composition with respect to K^+ and Na^+ concentrations was maintained in FAc-poisoned rabbit kidney slices.[58]

Apical Structures

There was no morphologic evidence to suggest that pinocytotic activity was impaired throughout poisoning *in vivo*. Some focal losses of brush border occurred in S_1 tubules where the RER was grossly vacuolated but apical dense tubules and pinocytotic invaginations were maintained.

Grossly enlarged apical vacuoles, especially marked in S_1 tubules, occurred early after 20 mg/kg and their size increased over a 2-hour period, but comparable vacuolation occurred in only 2 of the rats given 3.5 mg/kg. Blood glucose levels were measured in a second series of rats after dosing with 3.5 mg/kg and 20 mg/kg and a marked hyperglycemia, with rises between 200 and 400%, was recorded in all rats during the 2-hour period after receiving 20 mg/kg, whereas significant rises dur-

ing the first 3 hours occurred in only 2 of the 8 rats that received 3.5 mg/kg. These experiments are described in detail elsewhere.[1] The results provide evidence that the enlarged apical vacuoles were related to an FAc-induced hyperglycemic phase. Indirect evidence suggests that some glucose is absorbed by pinocytosis in the proximal tubule.[59] Injection of large volumes of hypertonic glucose does increase the size and number of apical vacuoles, especially in S_1 tubules,[60] posing the question as to whether or not the enlarged apical vacuoles in FAc-poisoned cells were merely a physiologic expression of an hyperglycemic episode. However, administration of hypertonic glucose solutions to control rats by intraperitoneal, intravenous and subcutaneous routes, to raise blood glucose levels to approximate levels that occurred during FAc poisoning, did not result in grossly enlarged apical vacuoles, although some increase in size and number did occur in S_1 tubules.[1] It is probable that during FAc-induced hyperglycemia, resulting from PFK inhibition, glucose is reabsorbed in excessive amounts from the tubular lumen by pinocytosis and an increase in the size and number of apical vacuoles would be an expression of a physiologic process and would be most marked in S_1 tubules. If PFK is inhibited in the kidney during the FAc-induced hyperglycemic phase, glucose catabolism may be decreased and the normal transport of glucose from vacuoles, as described in the ameba,[61] may be inhibited.

The hypothesis proposed is that the increased apical vacuolation in S_1 tubules during FAc-poisoning resulted from an increased glucose load in the glomerular filtrate, simultaneous with a decreased rate of glucose catabolism.

Endoplasmic Reticulum

Mitochondrial changes preceded dilatation of the RER. Moderate dilatation of the RER occurred early but the extensive dilatation that occurred at 12 and 24 hours was confined within the proximal tubule to S_1. The dilatation, which was progressive, was independent of cytoplasmic volume expansion and may not have resulted from the primary enzymic inhibition. The same change occurred in the RER of the thick ascending limb of Henle, the distal convoluted tubules and in the media of small arteries (interlobular) and arterioles.[1] With the exception of the vasculature, one function in common to the affected areas is active Na^+ transport,[62] and the cells are morphologically specialized for this function. Incorporation of abnormal fluorinated fatty acids derived from the metabolism of FAc [32] into the endoplasmic reticulum membrane may be involved, altering membrane function in some way and decreasing the

efficiency of a membrane-bound Na^+ pump. If this were so, accumulation of Na^+, together with water within the ER cisternae would be greatest in those cells specialized for Na^+ transport. The expansive property of the RER was quite remarkable, and the change appeared to be totally reversible. Extensive vacuolation of the RER was described in myocardial cultures during FAc poisoning.[63]

The Golgi Apparatus and Related Structures

The significance of the smooth-membrane ring forms with APase-positive cisternal contents is unknown. Morphologically similar forms were seen in S_1 cells during fluorocitrate and malonate poisoning.[1] The ring forms were quite common in FAc-poisoned S_1 cells but their absence from S_2 cells may have been a failure to observe them. Similar ring forms have been described near to the Golgi apparatus of normal cells.[25]

Autophagy of organelles [64] did not occur above the control level in poisoned cells. The demonstration of APase in small vacuolar bodies, spatially related to the Golgi apparatus, indicated that some, at least, were a type of lysosome but their site of origin was not confirmed. Hypertrophy of Golgi cisternae has been described in FAc-poisoned myocardial cultures [63] and, although hypertrophy was not observed in poisoned kidney cells, production of small vacuolar bodies may reflect increased Golgi activity. The Golgi apparatus represents at least one site of production of primary lysosomes.[65]

Cytosomes and Large Vacuolar Bodies

Despite a marked increase in the size of apical vacuoles in S_1 cells after 20 mg/kg, enlargement of cytosomes did not occur. When carbohydrates and other nonprotein substances are given in high doses, vacuolar changes occur in renal tubules. The ultrastructural features of this change, called "osmotic nephrosis," have recently been reviewed.[66] There is an increase in the number and size of apical vacuoles, a gradual accumulation of large pale cytoplasmic bodies and a simultaneous decrease in the number of dense cytoplasmic bodies. Superficially, tubular changes after 20 mg/kg (Fig 17) appeared similar to those occurring in "osmotic nephrosis," induced by intravenous injection of mannitol,[60] when the large vacuoles were thought to be altered cytosomes but those occurring during FAc poisoning were apical vacuoles.

It was clear that some cytosomes remained unchanged during poisoning, but the origin and nature of the large vacuolar bodies with dense "nucleoids," seen midcell in S_1 tubules, was not confirmed. The bodies shared features in common with dense cytosomes of normal cells and

they may have been derived from them (Fig 9 and 10). However, at 1 hour after 20 mg/kg, large numbers of vacuolar bodies and normal cytosomes were seen in the same cells, and it was impossible to know if they were altered cytosomes without labeling the cytosomes with a marker [64] before poisoning. Some of them may have arisen *de novo,* perhaps related to and derived from the small vacuolar bodies found near the Golgi apparatus. APase was not demonstrated in the large vacuolar bodies, but absence of activity does not confirm a nonlysosomal origin. APase was not demonstrated in all cytosomes in control cells, and if the matrix contents had been diluted, as suggested by their appearance, enzyme activity may have been below the threshold of sensitivity of the method used.

If the large vacuolar bodies were altered cytosomes, resulting from fusion with apical vacuoles, it is not clear why they did not enlarge to a size comparable with that of the apical vacuoles, as occurs during osmotic nephrosis. The significance of the bodies is not understood.

References

1. McDowell EM: An Ultrastructural and Histochemical Study of the Rat Kidney after *in vivo* Administration of Inhibitors of Krebs' Cycle. PhD thesis. University of Cambridge, 1971
2. Chenoweth MB: Monofluoroacetic acid and related compounds. Phamacol Rev 1:383–424, 1949
3. Buffa P, Peters RA: Formation of citrate *in vivo* induced by fluoroacetate poisoning. Nature 163:914, 1949
4. Buffa P, Peters RA: The *in vivo* formation of citrate induced by fluoroacetate and its significance. J Physiol (London) 110:488–500, 1949
5. Peters RA: Lethal synthesis. Croonian Lecture. Proc R Soc Lond [Biol] 139:143–170, 1952
6. Buffa P, Peters RA, Wakelin RW: Biochemistry of fluoracetate poisoning: isolation of an active tricarboxylic acid fraction from poisoned kidney homogenates. Biochem J 48:467–477, 1951
7. Lotspeich WD, Peters RA, Wilson TH: The inhibition of aconitase by "inhibitor fractions" isolated from tissues poisoned with fluoroacetate. Biochem J 51:20–25, 1952
8. Peters RA, Wakelin RW, Buffa P: Biochemistry of fluoroacetate poisoning: the isolation and some properties of the fluorotricarboxylic acid inhibitor of citrate metabolism. Proc R Soc Lond [Biol] 140:497–507, 1953
9. Maunsbach AB: The influence of different fixatives and fixation methods on the ultrastructure of rat kidney proximal tubule cells. II. Effects of varying osmolality, ionic strength, buffer system and fixative concentration of glutaraldehyde solutions. J Ultrastruct Res 15:283–309, 1966
10. Griffith LD, Bulger RE, Trump BF: The ultrastructure of the functioning kidney. Lab Invest 16:220–246, 1967
11. Yanoff M, Zimmerman LE, Fine BS: Glutaraldehyde fixation of whole eyes. Am J Clin Pathol 44:167–171, 1965

12. Klein RA: Histological Laboratory Methods. Edited by BP Disbrey, JH Rack. Edinburgh, ES Livingstone Publishers, 1970, p 124
13. Farquhar MG, Palade GE: Cell junctions in amphibian skin. J Cell Biol 26:263–291, 1965
14. Pease DC: Histological Techniques for Electron Microscopy. Second edition. New York, Academic Press Inc, 1964, p 260
15. Reynolds ES: The use of lead citrate at high pH as an electron-opaque stain in electron microscopy. J Cell Biol 17:208–212, 1963
16. Mercer EH, Birbeck MSC: Electron Microscopy; A Handbook for Biologists. Second edition. Oxford, Blackwell Scientific Publications, 1966, p 87
17. Maunsbach AB: Observations on the segmentation of the proximal tubule in the rat kidney: comparison of results from phase contrast, fluorescence and electron microscopy. J Ultrastruct Res 16:239–258, 1966
18. Bulger RE: The shape of rat kidney tubular cells. Am J Anat 116:237–255, 1965
19. Trump BF, Ericsson JLE: The effect of the fixative solution on the ultrastructure of cells and tissue: a comparative analysis with particular attention to the proximal convoluted tubule of the rat kidney. Lab Invest 14: 1245–1323, 1965
20. Trump BF, Bulger RE: Morphology of the kidney, Structural Basis of Renal Disease. Edited by EL Becker. New York, Harper & Row Publishers, 1968, pp 1–92
21. Ericsson JLE: Absorption and decomposition of homologous hemoglobin in renal proximal tubular cells: an experimental light and electron microscopic study. Acta Pathol Microbiol Scand: suppl 168:1–106, 1964
22. *Idem:* An electron microscopic and histochemical study of lysosomes in in the proximal tubules of rat kidney. J Histochem Cytochem 12:8–9, 1964
23. Ericsson JLE, Trump BF: Electron microscopic studies of the epithelium of the proximal tubule of the rat kidney. I. The intracellular localization of acid phosphatase. Lab Invest 13:1427–1456, 1964
24. Ericsson JLE, Trump BF, Weibel J: Electron microscopic studies of the epithelium of the proximal tubule of the rat kidney. II. Cytosegresomes and cytosomes; their relationship to each other and to the lysosome concept. Lab Invest 14:1341–1365, 1965
25. Ericsson JLE, Trump BF: Electron microscopic studies of the epithelium of the proximal tubule of the rat kidney. III. Microbodies, multivesicular bodies and the Golgi apparatus. Lab Invest 15:1610–1633, 1966
26. Maunsbach AB: Observations of the ultrastructure and acid phosphatase activity of the cytoplasmic bodies in rat kidney proximal tubule cells: with a comment on their classification. J Ultrastruct Res 16:197–238, 1966
27. Trump BF, Goldblatt PJ, Stowell RE: Studies of mouse liver necrosis *in vitro:* ultrastructural and cytochemical alterations in hepatic parenchymal cell nuclei. Lab Invest 14:1969–1999, 1965
28. Potter VR, Busch H, Bothwell J: Method for the study of tissue metabolism *in vivo* using fluoroacetate. Proc Soc Exp Biol Med 76:38–41, 1951
29. Potter VR, Busch H: Citric acid content of normal and tumour tissue *in vivo* following injection of fluoroacetate. Cancer Res 10:353–356, 1950
30. Lindenbaum A, White MR, Schubert J: Citrate formation *in vivo* induced by non-lethal doses of fluoroacetate. J Biol Chem 190:585–593, 1951

31. Gal EM, Peters RA, Wakelin RW: Some effects of synthetic fluoro-compounds on the metabolism of acetate and citrate. Biochem J 64:161–168, 1956
32. Gal EM, Drewes PA, Taylor NF: Metabolism of fluoroacetic acid-2-C^{14} in the intact rat. Arch Biochem 93:1–14, 1961
33. Gordon EE: The metabolism of citrate C^{14} in normal and in fluoroinhibitor poisoned rats. J Clin Invest 40:1719–1726, 1961
34. Crawford MA: The effects of fluoroacetate, malonate and acid-base balance on the renal disposal of citrate. Biochem J 88:115–120, 1963
35. Spencer AF, Lowenstein JM: Citrate content of liver and kidney of rat in various metabolic states and in fluoroacetate poisoning. Biochem J 103:342–348, 1967
36. Stoner HB: Studies on the mechanism of shock: the effect of trauma on the toxicity of 3-5 dinitrophenol-o-cresol and sodium fluoroacetate. Br J Exp Pathol 50:277–284, 1969
37. Morrison JF, Peters RA: The biochemistry of fluoroacetate poisoning; the effect of fluorocitrate on purified aconitase. Biochem J 58:473–479, 1954
38. Peters RA: Lethal synthesis and carbon-fluorine compounds, Biochemical Lesions and Lethal Synthesis. Oxford, London, New York, Pergamon Press, 1963, p 88–130
39. Schneider WC, Striebich MJ, Hogeboom GH: Cytochemical studies. VII. Localization of endogenous citrate in rat liver fractions. J Biol Chem 222: 969–977, 1956
40. Buffa P: Personal communication, 1969
41. Corsi A, Granata AL: Differential toxicity of fluoroacetate to heart, kidney and brain mitochondria of the living rat. Biochem Pharmacol 16:1083–1089, 1967
42. Buffa P, Azzone GF, Carafoli E, Muscatello V: Modificazioni biochimiche mitochondriali e tessutali in relazione ad alcune ipo-ed ipertermie sperimentali del ratto. Sperimentale 110:79–107, 1960
43. Margreth A, Azzone GFA: Respiration in fluoroacetate poisoned muscles. Biochem J 92:73–82, 1964
44. Elliott WB, Phillips AH: Effect of fluoroacetate on glucose metabolism *in vivo*. Arch Biochem 49:389–395, 1954
45. Engel FL, Hewson K, Cole BT: Carbohydrate and ketone body metabolism in the sodium fluoroacetate poisoned rat: "SFA diabetes." Am J Physiol 179:325–332, 1954
46. Bowman RH: Inhibition of citrate metabolism by sodium fluoroacetate in the perfused rat heart and the effect on phosphofructokinase activity and glucose utilization. Biochem J 93:13c–15c, 1964
47. Williamson JR, Jones EA, Azzone GF: Metabolic control in perfused rat heart during fluoroacetate poisoning. Biochem Biophys Res Commun 17: 696–702, 1964
48. Williamson JR: Glycolytic control mechanisms. III. Effects of iodoacetamide and fluoroacetate on glucose metabolism in the perfused heart. J Biol Chem 242:4476–4485, 1967
49. Goodwin TW: The Metabolic Roles of Citrate. Biochemical Society Symposia No. 27, Oxford, July, 1967. Edited by TW Goodwin. New York, Academic Press Inc, 1968
50. Greville GD: Intracellular compartmentation in the citric acid cycle, Citric

Acid Cycle. Edited by JM Lowenstein. New York, Marcel Dekker Inc, 1969, pp 1–119

51. Lehninger AL: Water uptake and extrusion by mitochondria in relation to oxidative phosphorylation. Physiol Rev 42:467–517, 1962
52. Parsons DF: Recent advances correlating structure and function in mitochondria. Int Rev Exp Pathol 4:1–54, 1965
53. Roodyn DB: The mitochondrion. Enzyme Cytology. Edited by DB Roodyn. New York, Academic Press Inc, 1967, pp 103–180
54. Pasquali-Ronchetti I, Greenawalt JW, Carafoli E: On the nature of the dense matrix granules of normal mitochondria. J Cell Biol 40:565–568, 1969
55. Trump BF, Ericsson JLE: Some ultrastructural and biochemical consequences of cell injury, The Inflammatory Process. Edited by BW Zweifach, L Grant, RT McCluskey. New York, Academic Press Inc, 1965, pp 35–120
56. Luft R, Ikkos D, Palmieri G, Ernster L, Afzelius B: A case of severe hypermetabolism of non-thyroid origin with a defect in the maintenance of mitochondrial respiratory control; a correlated clinical, biochemical and morphological study. J Clin Invest 41:1776–1804, 1962
57. Dick DAT: Relation between water and solutes: theory of osmotic pressure, Cell Water. Butterworths Molecular Biology and Medicine Series. London, Butterworth & Co Publishers, 1966, pp 15–43
58. Mudge GH: Electrolyte and water metabolism of rabbit kidney slices: effect of metabolic inhibitors. Am J Physiol 167:206–223, 1951
59. Caulfield JB, Trump BF: Correlation of ultrastructure with function in rat kidney. Am J Pathol 40:199–218, 1960
60. Maunsbach AB, Madden SC, Latta H: Light and electron microscopic changes in proximal tubules of rats after administration of glucose, mannitol, sucrose or dextran. Lab Invest 11:421–432, 1962
61. Chapman-Andresen C, Holter H: Studies on the ingestion of C^{14}-glucose by pinocytosis in the amoeba Chaos chaos. Exp Cell Res: Suppl 3:52–63, 1955
62. Pitts RF: Physiology of the Kidney and Body Fluids. An Introductory Text. Chicago, Yearbook Medical Publishers Inc, 1963, pp 91–115
63. Bovis R, Kasten FH, Okigaki T: Electron microscopic study of the toxic effect of sodium fluoroacetate on rat myocardial cultures. Exp Cell Res 43: 611–621, 1966
64. Ericsson JLE: Mechanism of cellular autophagy, Lysosomes in Biology and Pathology, Vol 2. Edited by DT Dingle, HB Fell. Amsterdam, London, North Holland Publishing Co, 1969, pp 345–394
65. Beams HW, Kessel RG: The Golgi apparatus: structure and function. Int Rev Cytol 23:209–276, 1968
66. Maunsbach AB: Functions of lysosomes in kidney cells,[64] Vol 1, pp 115–154

The sample of sodium fluoroacetate was kindly donated by Professor P. Buffa.

Legends for All Figures

Fig 1–4 are light micrographs of 0.5–1.0 μ thick sections of Araldite-embedded tissue, stained with alkaline toluidine blue solution.

Fig 1—Control. The brush border of the neck (*N*) and S_1 (*1*) is long and slender mitochondria can be seen lying perpendicular to the basement membrane. There is no difference in the degree of apical vacuolation between S_1 and S_2 (*2*) tubules. S_2 is recognizable in male rats by numerous large dense cytoplasmic bodies. Dense cytoplasmic bodies are much smaller in S_1 (*arrow*). Nuclei are round or elliptical and dense stained chromatin aggregates and nucleoli can be seen (× 1000).

Fig 2—1 hour after 20 mg/kg FAc. Numerous enlarged vacuoles are seen in the neck (*N*) and S_1(*1*). Small dense cytoplasmic bodies are seen as in control cells but, in addition, mid-cell vacuolar bodies with dense "nucleoids" surrounded by a lighter area are present (*arrows*). In other respects, the cells look normal (× 1000).

Fig 3—2 hours after 20 mg/kg FAc. Section at the corticomedullary junction: S_1 (*1*) and S_2 (*2*) tubules are seen, representative of the cortical proximal convolutions and in addition, segments of the descending part (*3*) are present. Apical vacuoles are large in S_1 and extend up to 3 deep in the cells. Mid-cell vacuolar bodies are seen but normal dense cytoplasmic bodies are also present (*arrow*). Apical vacuolation is increased in S_2 but the vacuoles are smaller than in S_1 and are confined to the cell apices. Apical vacuolation is increased to a lesser extent in the descending part (× 400).

Fig 4—12 hours after 3.5 mg/kg FAc. Section at the corticomedullary junction. Vacuolation is marked in focal areas of the cytoplasm of the neck (*N*) and S_1 (*1*) but vacuolation is absent from S_2 (*2*) and the descending part (*3*). Brush border is largely retained but is lost from focal areas of S_1 (*arrow*), that are not vacuolated. Vacuolation is marked in the distal tubules (*D*) and less marked in the thick ascending limbs of Henle (*H*) (× 400).

Fig 5–21 are electron micrographs of S_1 tubules. All tissue was stained *en bloc* with uranyl acetate. Sections were stained on grids with lead citrate.

Fig 5—Control. Typical appearance of an S_1 tubule. Apical tubular invaginations are present at the bases of the microvilli (*top right*) and many apical vesicles are present in the apical cytoplasm. Large apical vacuoles (*AV*) are seen below them and some dense material is present towards the periphery of one of them (*arrow*). Several dense cytosomes (*C*) are seen. The mitochondrial matrix has considerable electron density. Ribosomes in polysome groups are scattered in the cytoplasm and small chains of rough endoplasmic reticulum are present; the cisternae are not dilated. The nuclear chromatin is clumped, the perinuclear cisterna is not dilated (× 12,000).

Fig 6—Control. Long mitochondria lie within cytoplasmic interdigitations; dense matrix granules are present and the matrix has considerable electron density. Ribosomes are in polysome groups and the cisternae of small chains of rough endoplasmic reticulum are not dilated (*small arrows*). The cytosome is surrounded by a single membrane and within the dense matrix there are focal areas of increased density and some peripheral layered material (*large arrow*). G indicates Golgi apparatus (× 27,000).

Fig 7—1 hour after 20 mg/kg FAc. The mitochondrial matrix has low electron density and matrix granules are absent but the mitochondria are not swollen (compare with control, Fig 6). The normal arrangement of cristae is largely retained but in some mitochondria the cristae appear angulated (*arrows*). Ribosomes are in polysome groups. *BM* indicates basement membrane (× 27,000).

Fig 8—1 hour after 20 mg/kg FAc. Three large apical vacuoles are in fusion but otherwise, apical structures appear normal. Single-membrane-bounded bodies with floccular contents and a few small vesicles are associated and appear to be fusing with the vacuoles (*large arrow*). Small vacuolar bodies (*small arrows*) are seen in the apical cytoplasm. The cisternae of the rough endoplasmic reticulum are moderately dilated and the content has low electron density. A normal cytosome (C) is present (× 20,000).

Fig 9—1 hour after 20 mg kg FAc, neck segment. Large apical vacuoles are present (*AV*). A large single-membrane-bounded vacuolar body (*V*) is seen midcell. A central dense "nucleoid" is surrounded by an outer zone of loose floccular material, the whole surrounded by an electron-translucent zone. Focal areas of increased density are seen in the "nucleoid." The Golgi apparatus (G) appears normal but spatially related to it is a small vacuolar body (*small arrow*) and a ring form (*rf*), enclosing cytoplasm and ribosomes. The rough endoplasmic reticulum is moderately dilated (*large arrow*). A cytosome (C) appears normal (× 39,000).

Fig 10—90 minutes after 20 mg/kg FAc. Apart from the presence of large apical vacuoles, apical structures (*top left*) appear normal. Two large vacuoles are fusing and are closely associated with a large vacuolar body (*V*) characterized by a dense central zone or "nucleoid" surrounded by a translucent zone with floccular contents. Membranous material within the body suggests that it is an altered cytosome. The ribosomes are dispersed (× 20,000).

Fig 11—1 hour after 20 mg/kg FAc. A large apical vacuole (*AV*) contains a small amount of peripherally placed dense material. Acid phosphatase activity is demonstrated in the cytosome (*large arrow*) but is absent from the large vacuolar body (*center*). × 33,000.

Fig 12—90 minutes after 20 mg/kg FAc. Acid phosphatase activity is demonstrated in a cytosome but not in the single-membrane-bounded body with pale contents, within which lie a few vesicles (*arrow*), which is closely associated with an apical vacuole (*AV*) (× 26,000).

Fig 13—90 minutes after 20 mg/kg FAc. A group of small vacuolar bodies at midcell; each is bounded by a single membrane and has a matrix of moderate electron density, surrounded by an electron translucent zone. Two large vacuolar bodies (*V*) are present. Golgi apparatus (G) (× 26,000).

Fig 14—1 hour after 20 mg/kg FAc. Acid phosphatase activity is demonstrated in some of the small vacuolar bodies at midcell level (*arrows*). *AV* indicates apical vacuoles (× 21,500).

Fig 15—1 hour after 20 mg/kg FAc. Acid phosphatase activity is demonstrated within the cisterna of a ring form spatially related to the Golgi apparatus. Some enzyme activity is located within the Golgi cisternae (× 40,000).

Fig 16—1 hour after 20 mg/kg FAc. Acid phosphatase activity in the cisterna of a ring form in the apical cytoplasm; enzyme activity is also demonstrated in a small vacuolar body (*arrow*) (× 45,000).

Fig 17—2 hours after 20 mg/kg FAc. The brush border appears normal and apical tubular invaginations are seen between the bases of the microvilli. Very large apical vacuoles lie three-deep in the cell, two are in fusion (*arrow*). Normal cytosomes persist (C). The ribosomes are scattered but the nucleus appears as in control cells (× 13,000).

Fig 18—3 hours after 3.5 mg/kg FAc. Midcell vacuolar bodies, small (*arrow, top left*) and large (*arrow, center*), are present. The vacuolar profiles containing sparse floccular material represent dilatations of the rough endoplasmic reticulum; ribosomes have largely been dislocated but a few remain membrane bound (*small arrow*). The ribosomes are scattered free in the cytoplasm. The mitochondria are very swollen but retain their elongated form and the cristae persist (× 17,500).

Fig 19—24 hours after 3.5 mg/kg FAc. The brush border is absent over this focal area of vacuolation. Small vacuolar bodies are seen in the apical cytoplasm. The Golgi cisternae (G) are not dilated despite extensive dilatation of the endoplasmic reticulum. Sparse floccular material is seen in the dilatations. The mitochondria are not swollen but matrix granules are absent. The cytoplasmic volume is normal and polysome groups are present in cells where dilatation is less marked (*lower left*) but ribosomes are scattered in the vacuolated cells. Small lipid droplets (*l*) are seen at the cell base (× 17,000). **Inset**—12 hours after 3.5 mg/kg FAc. Dilatation of the rough endoplasmic reticulum and focal dilatation of the nuclear envelope (× 9000).

Fig 20—24 hours after 3.5 mg/kg FAc. The rough endoplasmic reticulum is not dilated in these S_1 cells and apart from absence of mitochondrial matrix granules, the cells appear normal (× 29,000).

Fig 21—48 hours after 3.5 mg/kg FAc. Abnormal matrix inclusion bodies are present in some mitochondria (*arrows*). The electron density of the matrix is reduced and the mitochondria are a little swollen. In all other respects, the cells appear normal (× 29,000).

1

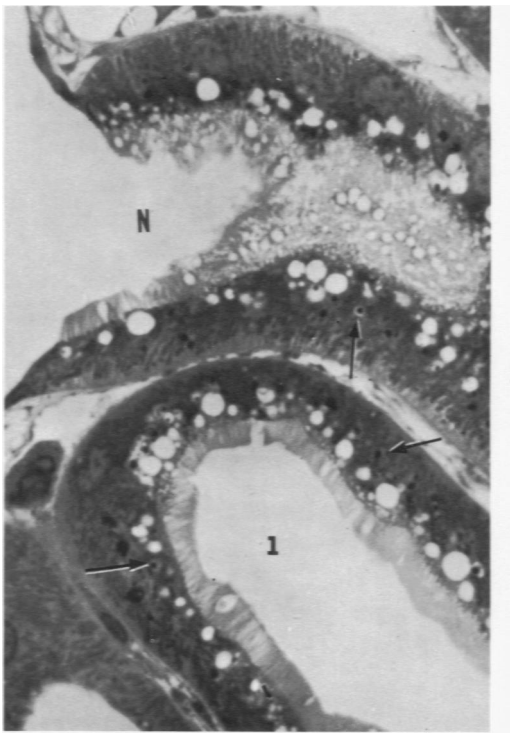

2

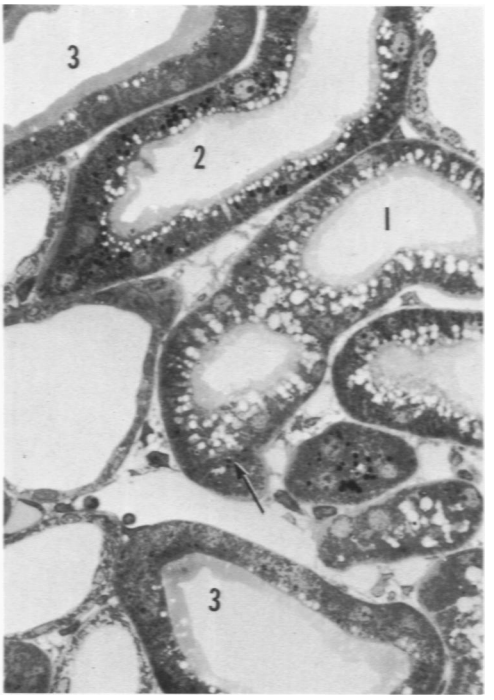

3

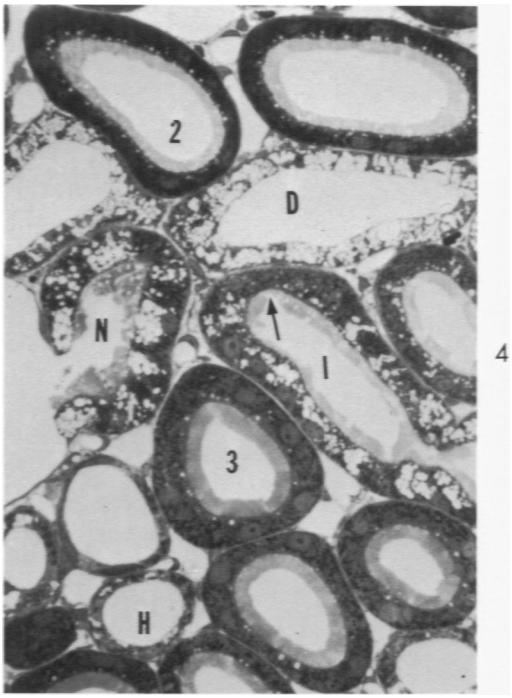

4

5

6

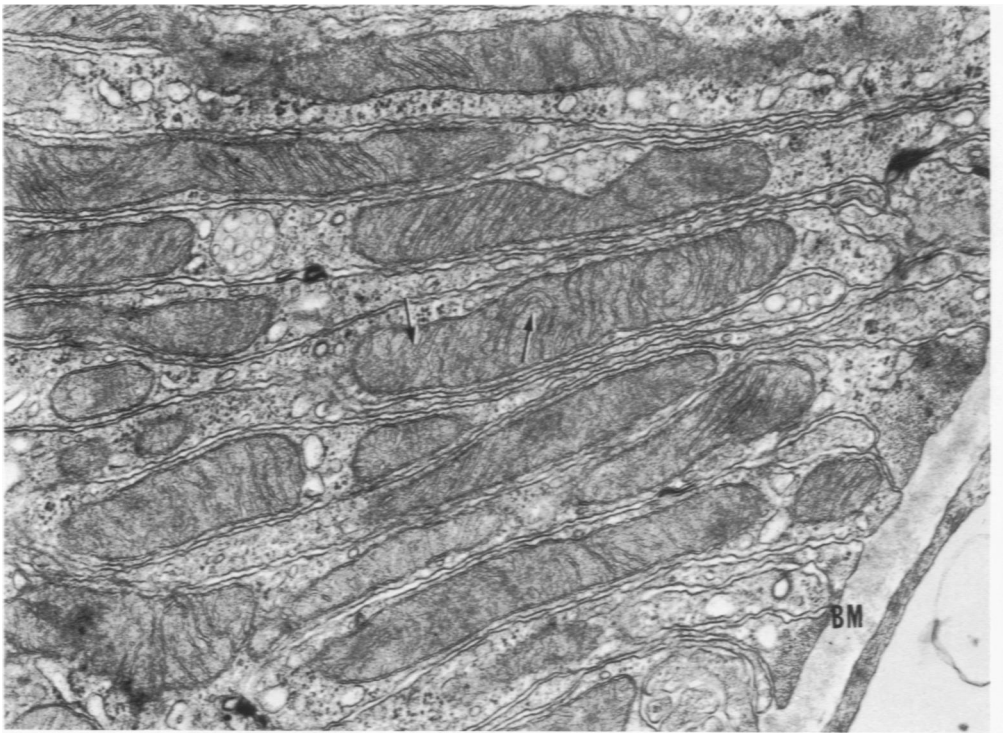

7

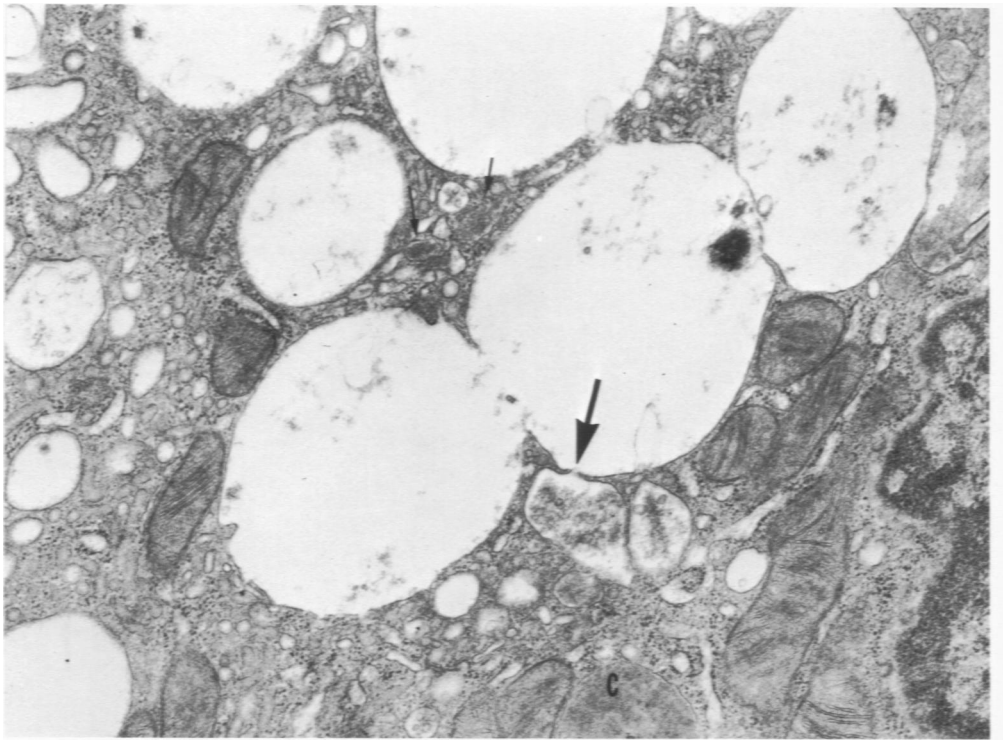

8

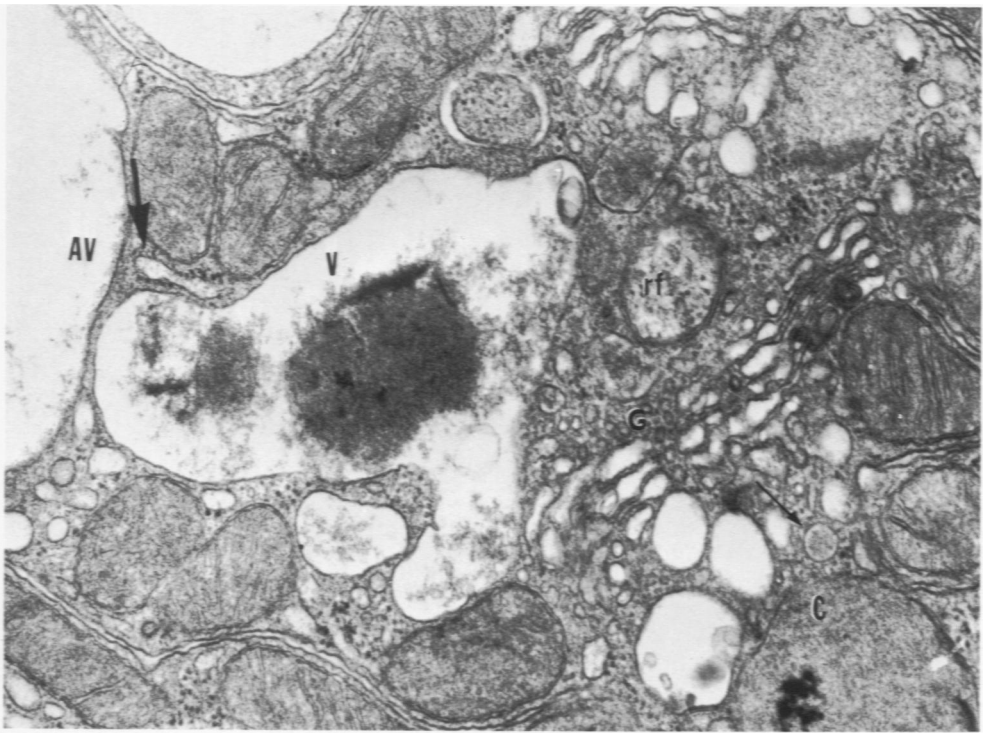

9

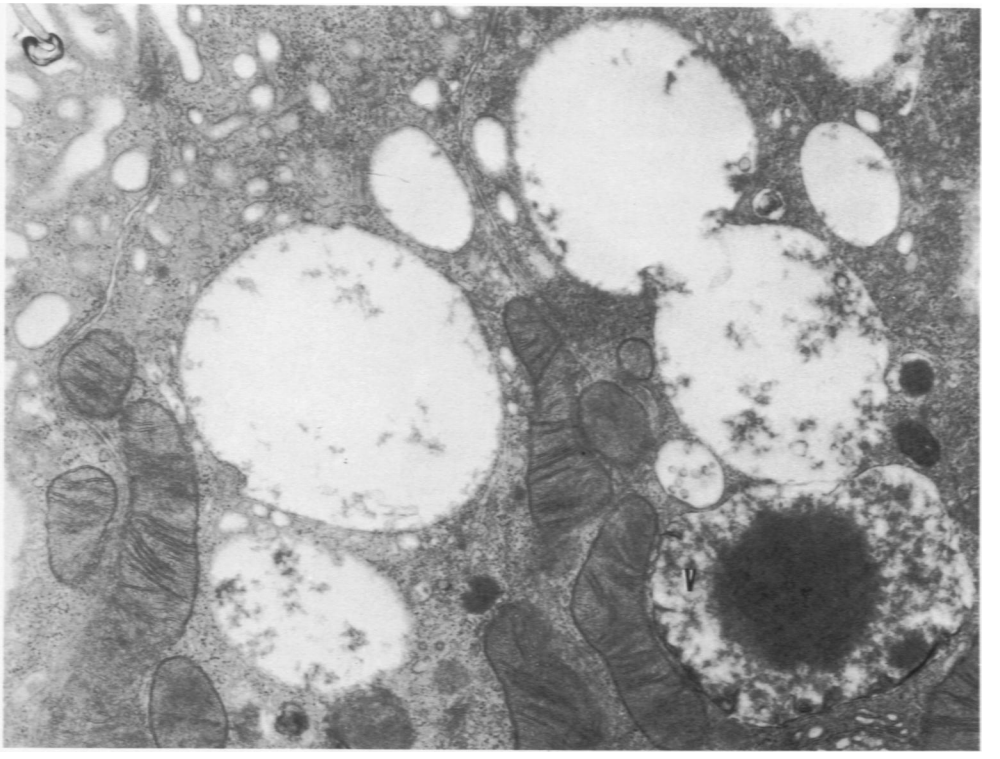

10

11

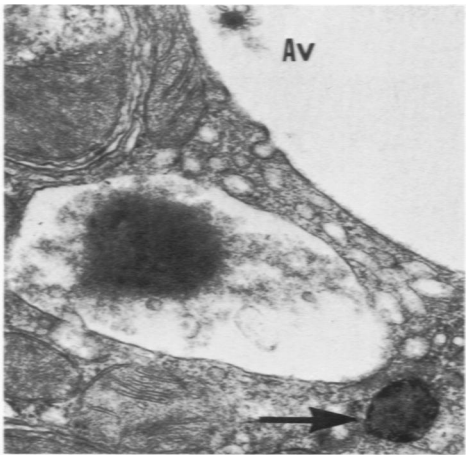

12

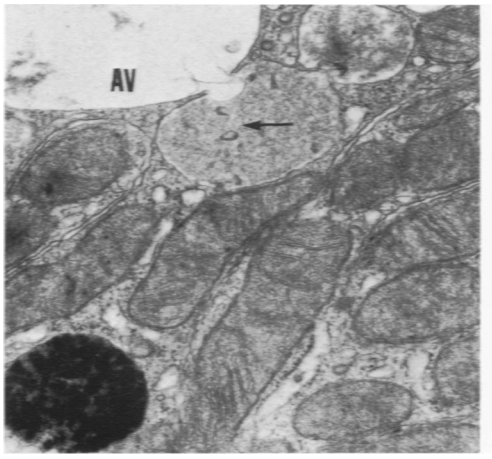

13

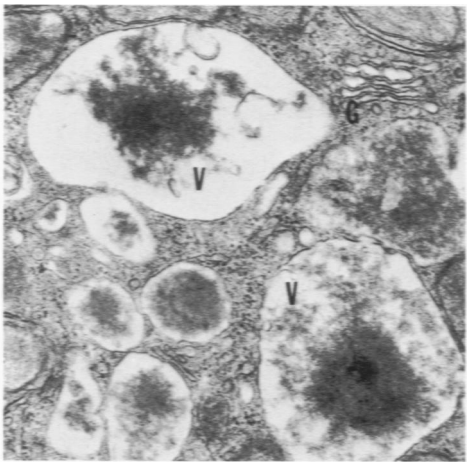

14

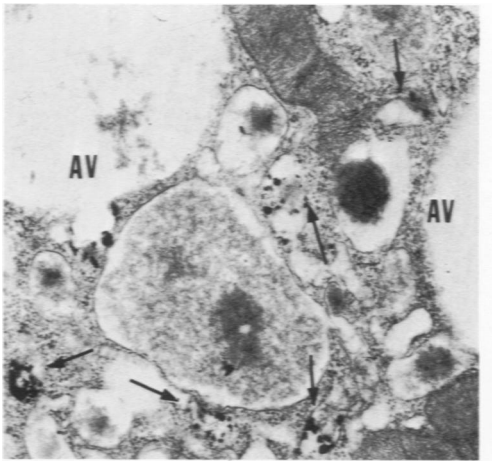

15

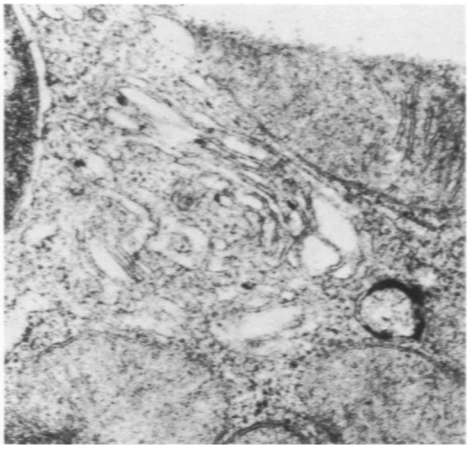

16

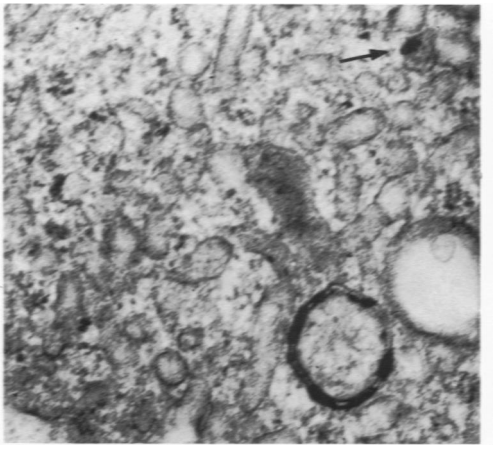

17

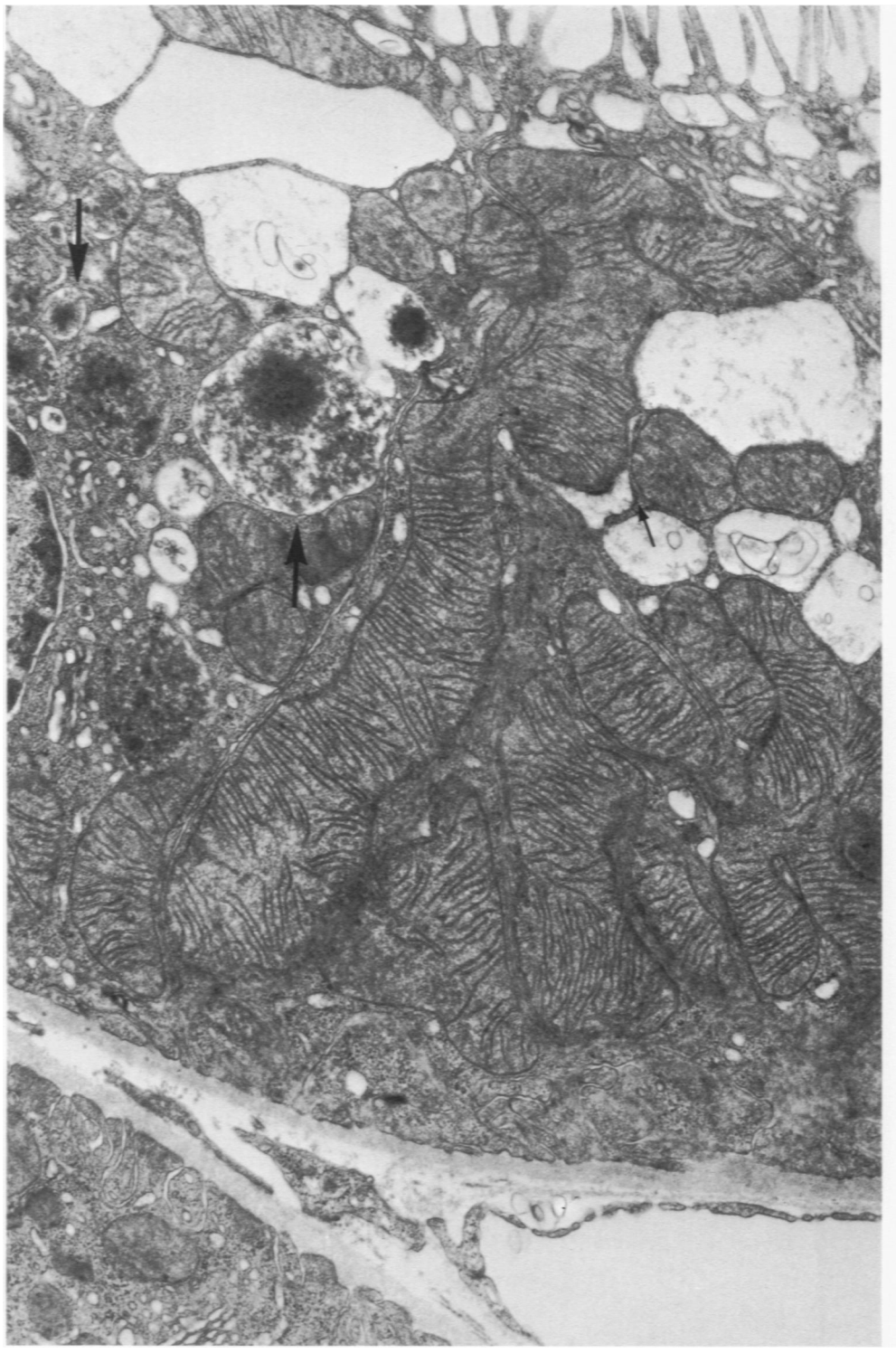

18

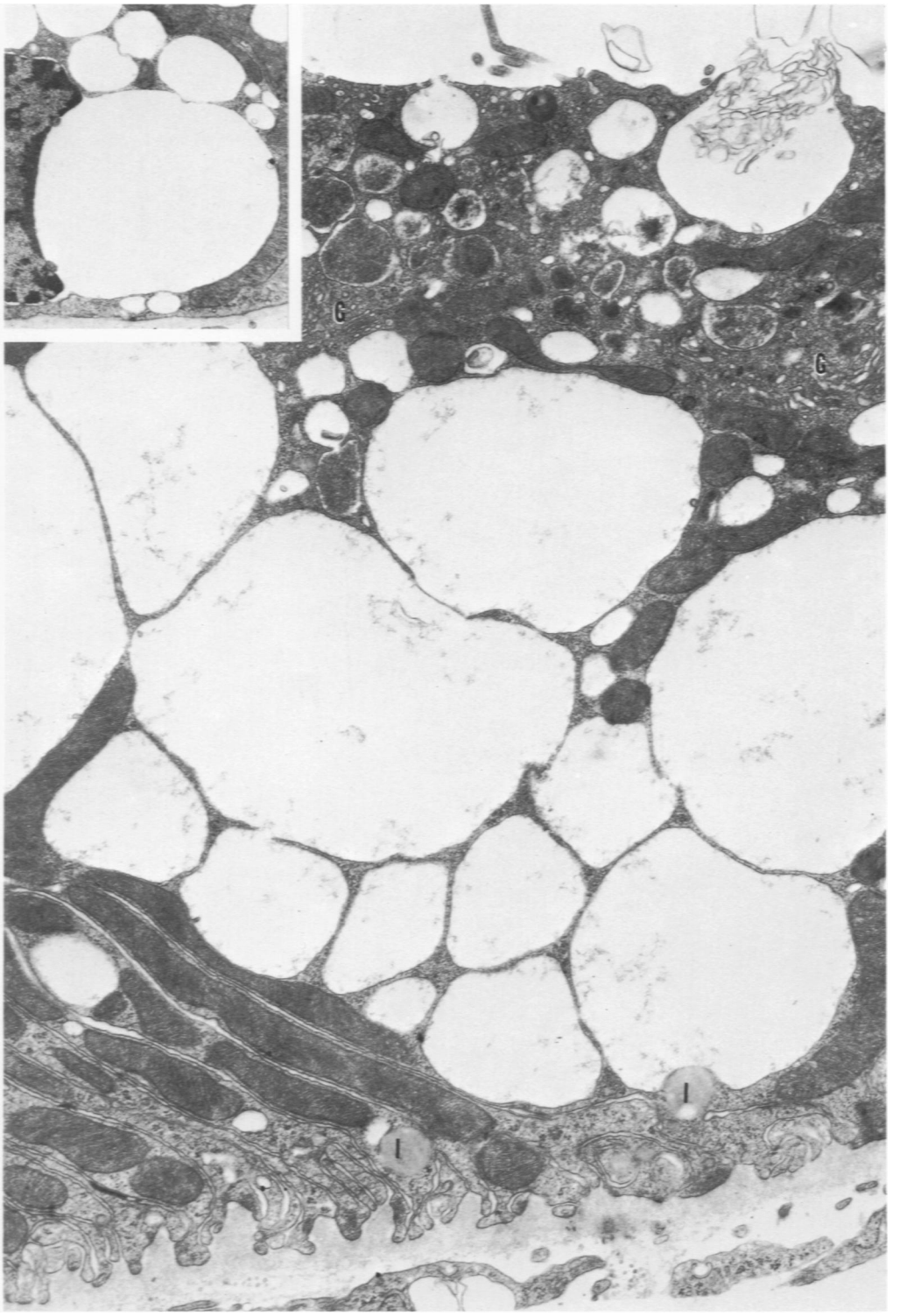

19

20

21

[*End of Article*]